

AD-A051 303

NAVAL RESEARCH LAB WASHINGTON D C
STUDIES OF ION BEAM GENERATION EFFICIENCY WITH REFLEX TETRODES. (U)

F/G 20/7

JAN 78 R A MAHAFFEY, J A PASOUR, J GOLDEN

NRL-MR-3694

SBIE-AD-E000 119

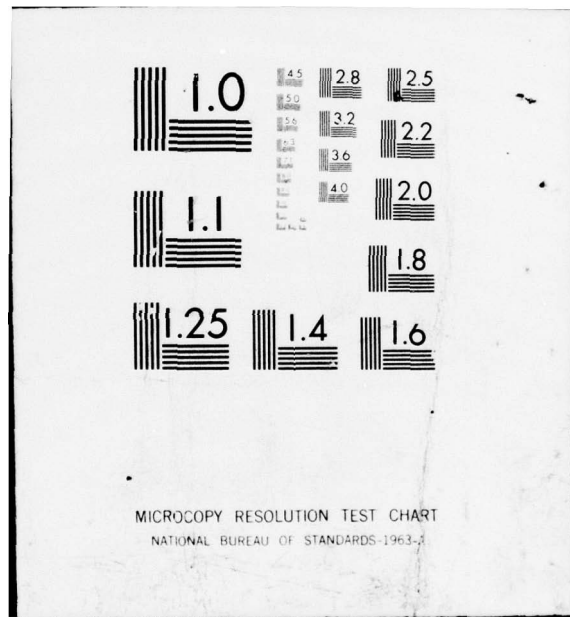
NL

UNCLASSIFIED

| QF |
AD
A051303



END
DATE
FILED
4-78
DDC



AD A 051303

ade 00019
NRL Memorandum Report 3694

Studies of Ion Beam Generation Efficiency With Reflex Tetrodes

R. A. MAHAFFEY, J. A. PASOUR, J. GOLDEN and C. A. KAPETANAKOS

Experimental Plasma Physics Branch
Plasma Physics Division

12

AD No.
DDC FILE COPY

January 1978

D D C
RECEIVED
MAR 16 1978
REFUGUEE B



NAVAL RESEARCH LABORATORY
Washington, D.C.

Approved for public release; distribution unlimited.

REPORT DOCUMENTATION PAGE			READ INSTRUCTIONS BEFORE COMPLETING FORM
1. REPORT NUMBER NRL Memorandum Report 3694	2. GOVT ACCESSION NO.	3. RECIPIENT'S CATALOG NUMBER 9	4. TYPE OF REPORT & PERIOD COVERED Interim report on a continuing NRL problem.
4. TITLE (and Subtitle) STUDIES OF ION BEAM GENERATION EFFICIENCY WITH REFLEX TETRODES.	5. PERFORMING ORG. REPORT NUMBER 10		6. CONTRACT OR GRANT NUMBER(s) 16 RR01109
7. AUTHOR(s) R. A. Mahaffey, J. A. Pasour*, J. Golden, C. A. Kapetanakos	8. PERFORMING ORGANIZATION NAME AND ADDRESS Naval Research Laboratory Washington, D. C. 20375 17 RR0110942		9. PROGRAM ELEMENT, PROJECT, TASK AREA & WORK UNIT NUMBERS see reverse side for data NRL Problem H02-28A 10/17/75
11. CONTROLLING OFFICE NAME AND ADDRESS Office of Naval Research Arlington, Virginia 22217	12. REPORT DATE January 1978 11		13. NUMBER OF PAGES 15
14. MONITORING AGENCY NAME & ADDRESS (if different from Controlling Office) 12 15p, 18 SBIE	15. SECURITY CLASS. (of this report) UNCLASSIFIED		16a. DECLASSIFICATION/DOWNGRADING SCHEDULE 19 AD-E000 119 D D C R-PAPRI/IR MAR 16 1978 19 AD-E000 119 D D C R-PAPRI/IR MAR 16 1978 B
16. DISTRIBUTION STATEMENT (of this Report) Approved for public release; distribution unlimited. 14 NRL-MR-3694	17. DISTRIBUTION STATEMENT (of the abstract entered in Block 20, if different from Report)		18. SUPPLEMENTARY NOTES This research was supported by the Office of Naval Research and the Department of Energy. *NRC Research Associate at Naval Research Laboratory.
19. KEY WORDS (Continue on reverse side if necessary and identify by block number) Intense ion sources Reflex tetrode Reflex triode Ion beams	20. ABSTRACT (Continue on reverse side if necessary and identify by block number) The unidirectionality of the ion current in a reflex tetrode has as a result the efficient generation of pulsed, ion beams. In this paper, experimental results are reported on the dependence of the ion generation efficiency, in a reflex tetrode, upon the applied voltage, total current, anode-anode and anode-cathode separations and applied magnetic field.		

251 950

1B

Preceding Page BLANK - FILMED

STUDIES OF ION BEAM GENERATION EFFICIENCY WITH REFLEX TETRODES

I. INTRODUCTION

Recently, low inductance, coaxial reflex triodes have been used on the Gamble II accelerator at NRL to produce proton beams with currents in excess of 200 kA¹. Interest in the generation of intense ion beams has been stimulated primarily by their potential applications. These applications include the production of field-reversed ion rings², inertial confinement fusion³, laser excitation⁴, hybrid reactors⁵, and plasma heating⁶.

Among the various ion sources presently available, the reflex triode^{1,7} has several attractive features. Reflex triodes can operate over a wide range of applied axial magnetic field and the ion current produced by a reflex triode can be considerably higher than that predicted for bipolar flow. The reflex triode has the undesirable feature, however, that about one half of the ion current flows toward the real cathode and is unusable. Under ideal conditions, therefore, the maximum efficiency of a reflex triode cannot exceed 50%. In practice, the efficiency of reflex triodes is < 30%.

Various attempts have been made to increase the efficiency of reflex triodes. These include attempts to suppress the backward flowing ion current by using a compound anode^{8,9} and to delay the impedance collapse⁸ by using an anode that is radially displaced from the cathode. These attempts have resulted in only modest increases in efficiency and poor shot-to-shot reproducibility.

Recently, however, a new configuration¹⁰ (called the reflex tetrode) has been developed. This device (obtained by adding a second anode to a reflex triode) preserves the advantages of a reflex triode while reducing the wasted ion current which flows toward the real cathode to < 2%. This reduction in backward streaming ion current in a reflex tetrode¹⁰ results in a large improvement in proton production efficiency. The maximum efficiency under ideal conditions

Note: Manuscript submitted January 10, 1978.

Section	<input checked="" type="checkbox"/>	
Section	<input type="checkbox"/>	
BY		
DISTRIBUTION/AVAILABILITY CODES		
Dist.	AIL	and/or SPECIAL
A		

may approach 100%. In addition, impedance collapse is reduced since there are few backstreaming ions to enhance the cathode emission.

This letter reports on various factors which can influence the proton generation efficiency in reflex tetrodes, including applied voltage, total current, anode-anode separation, anode thickness, anode-cathode gap, and the applied axial magnetic field.

II. EXPERIMENT

A schematic of the reflex tetrode experiment is shown in Fig. 1. A 5-cm diam. graphite cathode which is at ground potential is located a distance A_1-K from the first anode, A_1 . This anode foil is either a 2- μm -thick polycarbonate (kimfol) or a 6 or 12- μm -thick aluminized mylar foil. The second anode, A_2 , is placed a distance A_1-A_2 from A_1 toward the virtual cathode and is made of 13- μm -thick polyethylene foil. The primary source of protons is the polyethylene anode (A_2) as aluminized mylar or kimfol anodes have been observed to be poor sources of protons in previous reflex triode experiments.¹¹ Anodes A_1 and A_2 are at the same electrical potential. The hypothesized electric potential of this configuration is shown in Fig. 1. This potential results in the suppression of the ion flow in the A_1-K gap. The anodes are mounted on the edges of a 12.7 cm I.D. aluminum ring. The ring is connected to the Seven Ohm Line (SOL) generator which is operated in positive polarity. The output voltage pulse of this generator has an amplitude U_0 and a duration of ≈ 50 nsec (FWHM). The experiments are performed with an applied axial magnetic field B_0 .

The number of protons emitted in either axial direction is determined by nuclear activation techniques¹². Thick carbon (C) or boron nitride (BN) targets are placed ≈ 7 cm from A_2 to determine the number of forward-directed protons. The number of back-directed protons is determined by measuring the

activity induced in the graphite cathode and on BN or carbon targets placed around the cathode. In cases where the proton flux is intense enough to cause substantial target blow off¹², a 33% transparent screen is placed in front of the target to reduce the number of protons striking the target.

Since nuclear activation gives only the time integrated proton yield, the proton current is inferred from the total yield together with the duration of the proton pulse. The duration of the proton pulse is assumed to be equal to the time interval from plasma formation until the diode voltage drops below the threshold for target activation (277 kV for the $^{14}\text{N}(\text{p},\gamma)^{15}\text{O}$ reaction on BN, 430 kV for the $^{12}\text{C}(\text{p},\gamma)^{13}\text{N}$ reaction on graphite). To determine the proton generation efficiency ϵ , the resulting average proton current is divided by the average value of the total current during this time (as measured with a resistive shunt in the outer conductor of the SOL generator).

The proton generation efficiency is graphed versus the average value of the shunt current for two values of the applied voltage in Figure 2. For these experiments, $B_0 \approx 5.6$ kG, $A_1-K \approx 1.7$ cm, A_1 is 6- μm -thick aluminized mylar and $A_1-A_2 \approx 0.5$ cm. As seen, for constant voltage, ϵ increases with the shunt current I . For constant current, ϵ increases with decreasing voltage. In addition, the proton generation efficiency for reflex triodes is approximately one half the efficiency of reflex tetrodes. The observed scaling, $\epsilon \sim I/U_0$, has also been observed for reflex triodes¹³. This scaling is apparently the result of the virtual cathode dependence on the system parameters. That is, the larger the number of oscillating electrons N_{osc} in the device ($N_{\text{osc}} \sim I$) or the lower the applied voltage (energy of electrons) the closer the virtual cathode forms to A_2 . A smaller distance between the virtual cathode and the anode results in a larger electric field on the side of A_2 toward the virtual cathode.

Thus, the observed dependance $\epsilon \sim I/U_o$ is expected.

Figure 3 shows schematically the dependence of the electric potential on the A_1-A_2 gap. If A_1-A_2 is too small (Fig. 3a), the tetrode's electric potential is similar to a reflex triode and little improvement over reflex triode operation is expected. If A_1-A_2 is made too large (Fig. 3c), it is possible that a virtual cathode is formed between the two anodes and thus electrons are unable to reach A_2 . Therefore, an optimum A_1-A_2 gap is likely. Experimentally, this is found to be the case as is illustrated in Fig. 4. In these experiments, $B_o \approx 5.6$ kG, $A_1-K \approx 1.7$ cm, A_1 is 6- μm -thick aluminized mylar, and $U_o \approx 490$ kV. Of the three A_1-A_2 gaps investigated, it is found that the tetrode with $A_1-A_2 \approx 0.5$ cm has slightly better efficiency than the tetrode with $A_1-A_2 \approx 1.1$ cm and much better efficiency than the tetrode with $A_1-A_2 \approx 0.2$ cm. In fact, when $A_1-A_2 \approx 0.2$ cm, ϵ is less than for a triode with $A-K \approx 2.3$ cm with a 13- μm -thick polyethylene anode. The reason for the low efficiency of the $A_1-A_2 \approx 0.2$ cm tetrode is that the electric potential is quite similar to that of a reflex triode, but now the total anode foil thickness is 19 μm . The effect of anode foil thickness on proton generation in a reflex triode has been previously reported ¹⁴. It was observed that when the anode foil thickness was increased from 13- μm to 19- μm that the proton production decreased about 15%. This is approximately the difference in efficiency between the reflex triode and reflex tetrode with $A_1-A_2 \approx 0.2$ cm seen in Fig. 4.

With a 2- μm -thick A_1 foil (whose thickness is small compared to the 8- μm range of 0.5 MeV protons), no radioactivity from backstreaming protons is detected on the cathode nor on BN targets placed around the cathode. Thus, the unidirectionality of the proton current is

evidently due solely to the electric potential distribution and not to stopping by A_1 . The effect of varying the thickness of A_1 is shown in Fig. 5. The efficiency of tetrodes with 2- μm or 6- μm -thick A_1 's is approximately the same, but the efficiency of a tetrode with 13- μm -thick A_1 is reduced by about 30%. This is due to the reduced number of electron transits which result when the total anode thickness is 25- μm instead of 19- μm or 15- μm . The two smaller anode thicknesses have been found to result in approximately the same number of protons emitted in earlier reflex triode studies.¹⁴

In the range $2.7 \text{ kG} \leq B_0 \leq 7.6 \text{ kG}$ operation of the reflex tetrode is found to be relatively independent of applied axial magnetic field. When $B_0 \sim 0$, however, proton generation efficiency is greatly reduced. This is attributed to electron losses and to two-dimensional effects associated with self-magnetic fields. These effects have been observed in reflex triode experiments.¹ In addition, the efficiency of the tetrode is found to be insensitive to the range $0.9 \text{ cm} \leq A_1\text{-K} \leq 1.9 \text{ cm}$.

III. SUMMARY AND CONCLUSION

The reflex tetrode is a device which resembles the reflex triode but includes a second anode that modifies the electric potential. Under proper operating conditions $\geq 98\%$ of the protons produced in the tetrode flow toward the virtual cathode and out of the device. Peak ion currents in excess of 10 kA (0.5 kA/cm^2) with $\approx 10^{15}$ protons have been detected on SOL. Impedance collapse in the tetrode is greatly reduced since there are very few backstreaming ions to enhance the cathode emission. Thus, a smaller $A_2\text{-K}$ gap can be used in the tetrode configuration than in the triode configuration. Proton generation efficiencies greater than 55% have been obtained, and it is observed that the efficiency is proportional to I/U_0 . The proton production efficiency for

reflex tetrodes is observed to be approximately twice the efficiency of reflex triodes under similar operating conditions.

In order to optimize reflex tetrode operation, it is necessary to have a thin A_1 and to have the proper A_1 - A_2 gap. For the experiments reported here, the best A_1 - A_2 gap is ≈ 0.5 cm, however, this value may differ at markedly different applied voltages.

It is observed that tetrode operation is not sensitive to B_0 in the range 2.7 kG $\leq B_0 \leq 7.6$ kG, however, $B_0 = 0$ results in poor operation of the device. In addition, variation in the anode-cathode gap results in little change in tetrode operation.

Experiments with small diameter cathodes (diam. ≈ 1.8 cm) with average electron current density as high as 2.5 kA/cm 2 indicate that reflex tetrodes can operate with high efficiency at the power level of the Gamble II generator. Therefore, usable proton currents in excess of 400 kA may be produced by converting the coaxial reflex triodes¹ used on the NRL Gamble II generator to coaxial reflex tetrodes.

The authors gratefully acknowledge the expert technical assistance of R. A. Covington.

References

1. J. Golden, C.A. Kapetanakos, S.J. Marsh, and S.J. Stephanakis, Phys. Rev. Lett. 38, 130 (1977).
2. C.A. Kapetanakos, J. Golden and F.C. Young, Nucl. Fus. 16, 151 (1976); C.A. Kapetanakos, J. Golden, Adam Drobot, R.A. Mahaffey, S.J. Marsh, and J.A. Pasour, 2nd Int'l. Top. Conf. on High Power Electron and Ion Beam Research and Technology, E2(1977); S. Humphries, Plasma Phys. 17, 973 (1975); and H.H. Fleischmann, Int'l Top. Conf. on Electron Beam Research and Technology 2, 129 (1975), for example.
3. M.J. Clauser, Phys. Rev. Lett. 35, 848 (1975); F. Winterberg, Nature 251, 44 (1974); and J. Shearer, Nucl. Fus. 15, 952 (1975) for example.
4. A.W. Ali, J. Golden, C.A. Kapetanakos, and R.W. Waynant, NRL Memo Report No. 3064 (1975); A.W. Ali and W.W. Jones, NRL Memo Report No. 3015 (1975); and J. Golden, R.A. Mahaffey, J.A. Pasour, A.W. Ali, W.W. Jones, and C.A. Kapetanakos, unpublished.
5. H.H. Fleischmann, Cornell Univ. LPS Report No. 186 (1976).
6. E. Ott and W.M. Manheimer, Nucl. Fus. 17, 1057 (1977).
7. S. Humphries, J.J. Lee, and R.N. Sudan, Appl. Phys. Lett. 25, 20 (1974); C.A. Kapetanakos, J. Golden, and W.M. Black, Phys. Rev. Lett. 37, 1236 (1976); and D.S. Prono, J.W. Shearer, and R.J. Briggs, Phys. Rev. Lett. 37, 21 (1976) for example.
8. Shyke A. Goldstein, J. Golden, R.A. Mahaffey, and Roswell Lee, IEEE Conference Record - Abstracts, Conf. on Plasma Science, 171 (1977).
9. S. Humphries, R.N. Sudan, and W.C. Condit, Appl. Phys. Lett. 26, 667 (1975).
10. J.A. Pasour, R.A. Mahaffey, J. Golden, and C.A. Kapetanakos, Phys. Rev. Lett. (1978), and NRL Memo Report No. 3670 Nov. (1977).

11. J. Golden, C.A. Kapetanakos, S.J. Marsh, and S.J. Stephanakis, NRL Memo Report No. 3422 (1976).
12. F.C. Young, J. Golden, and C.A. Kapetanakos, Rev. Sci. Inst. 48, 432 (1977).
13. R.A. Mahaffey, J.A. Pasour, J. Golden, and C.A. Kapetanakos, unpublished.
14. J. Golden, C.A. Kapetanakos, Roswell Lee and Shyke A. Goldstein, Int'l Top. Conf. Electron Beam Research and Technology 1, 635 (1975).

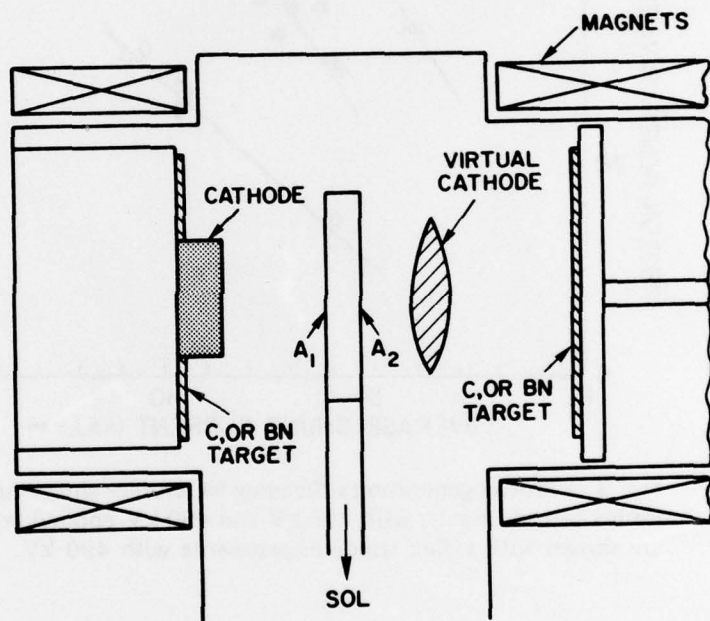
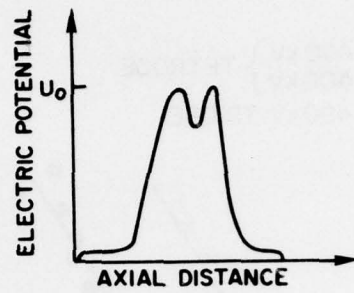


Fig. 1 — Schematic of the reflex tetrode experiment

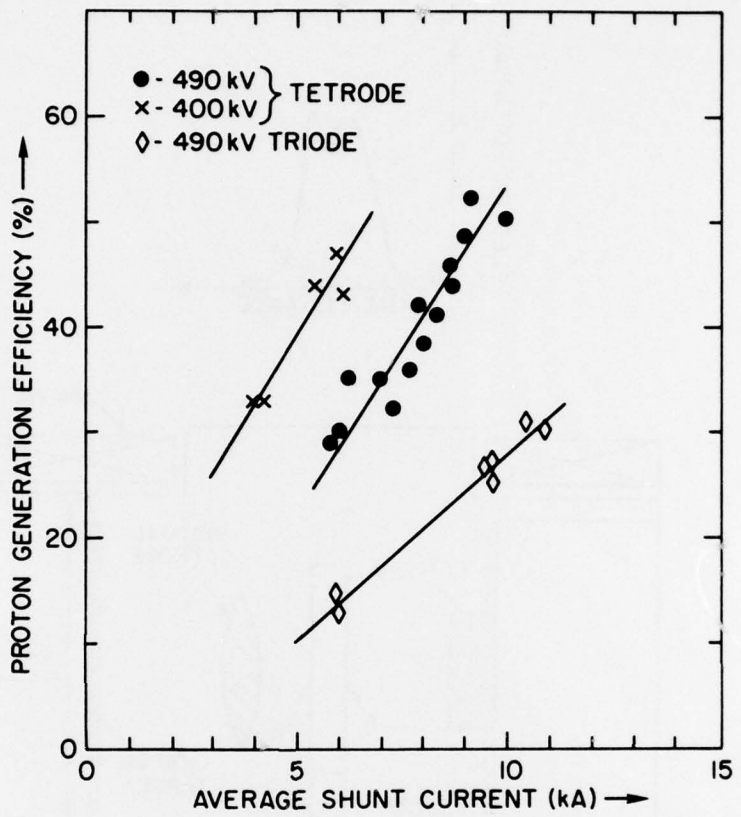


Fig. 2 — Proton generation efficiency vs. average shunt current. Reflex tetrode results with 400 kV and 490 kV applied voltages are shown with reflex triode experiments with 490 kV.

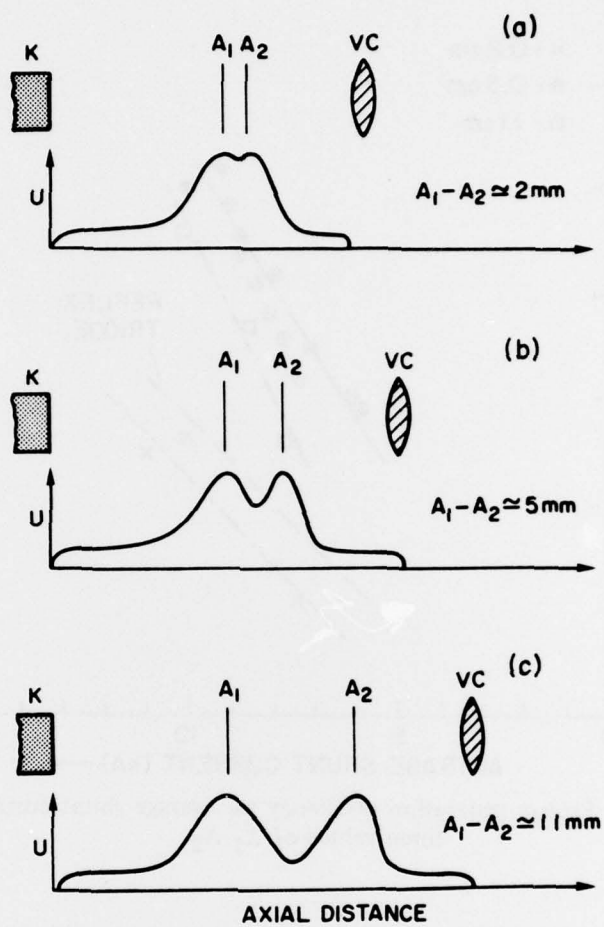


Fig. 3 — Variation of the hypothesized electric potential as the A_1 - A_2 gap is changed

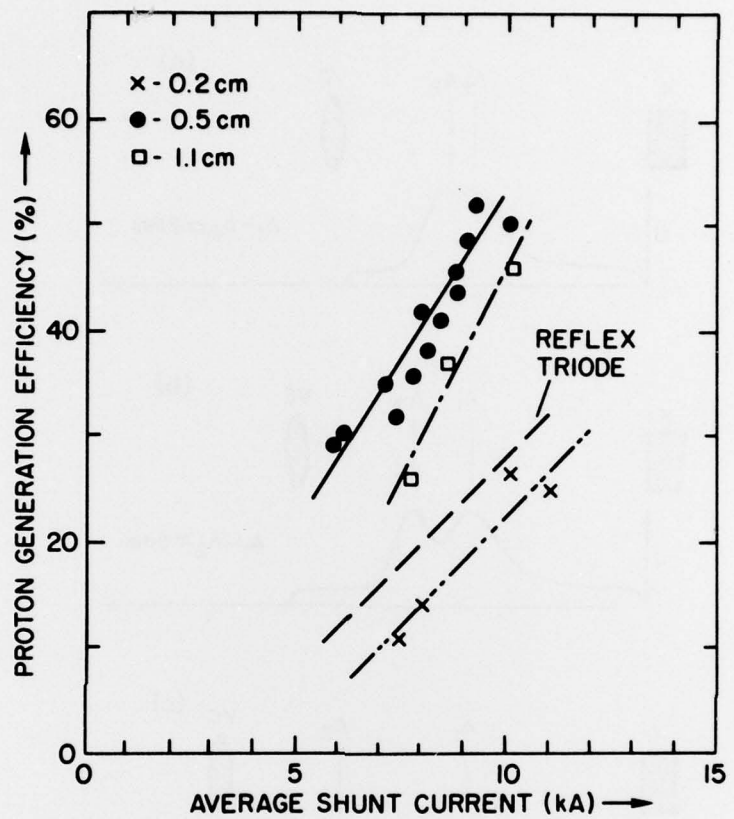


Fig. 4 — Proton generation efficiency vs. average shunt current for three values of $A_1 - A_2$

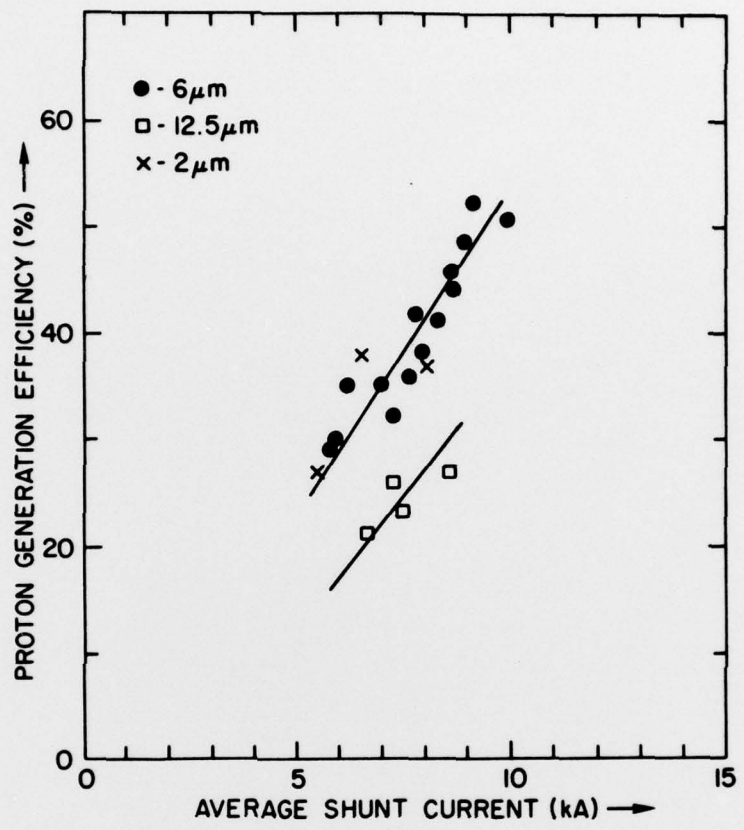


Fig. 5 — Proton generation efficiency vs. average shunt current for three thicknesses of A_1